RESEARCH ARTICLE | FEBRUARY 14 2023

# Numerical simulation of the combustion of preheated ultra-lean dimethyl ether/air mixture ⊘

Tomáš Blejchař ✉ ; Václav Nevrlý; Michal Dostál; Vít Klečka; Petr Bitala; Václav Válek; Michal Vašinek;
Jan Suchánek; Zdeněk Zelinger; Jan Wild

Check for updates

View Online

Export Citation

CrossMark

# Numerical Simulation of The Combustion of Preheated Ultra-Lean Dimethyl Ether/Air Mixture

Tomáš Blejchař[1, 2 a)], Václav Nevrlý[3, b)], Michal Dostál[3, 5, c)], Vít Klečka[3, d)], Petr Bitala[3, e)], Václav Válek[3, f)], Michal Vašinek[4, g)], Jan Suchánek[5, h)], Zdeněk Zelinger[5, i)] and Jan Wild[3, 6, j)]

[1]*Faculty of Mechanical Engineering, VSB-Technical University of Ostrava, 17.listopadu 15/2172, 708 00 Ostrava, Czech Republic*
[2]*IT4Innovations, VSB – Technical University of Ostrava,17. listopadu 15/2172, 70800 Ostrava, Czech Republic*
[3]*Faculty of Safety Engineering, VSB-Technical University of Ostrava, Lumírova 630/13, 700 30 Ostrava-Výškovice, Czech Republic*
[4]*Faculty of Electrical Engineering and Computer Science, VSB-Technical University of Ostrava, 17.listopadu 15/2172, 708 00 Ostrava-Poruba, Czech Republic*
[5]*J. Heyrovský Institute of Physical Chemistry, Czech Academy of Sciences, Dolejškova 2155/3, 182 23 Praha 8, Czech Republic*
[6]*Faculty of Mathematics and Physics, Charles University, Ke Karlovu 3, 121 16 Praha 2, Czech Republic*

[a)] *Corresponding author: tomas.blejchar@vsb.cz*

[b)]*vaclav.nevrlý@ vsb.cz,* [c)]*michal.dostal1@vsb.cz,* [d)]*vit.klecka@vsb.cz,* [e)]*petr.bitala@vsb.cz,* [f)]*vaclav.valek@vsb.cz,* [g)]*michal.vasinek@vsb.cz,* [h)]*jan.suchanek@jh-inst.cas.cz,* [i)]*zdenek.zelinger@jh-inst.cas.cz,* [j)]*jan.wild@vsb.cz*

**Abstract.** The combustion of preheated ultra-lean dimethyl ether/air mixture was investigated numerically. A laminar burner stabilized flame of preheated ultra-lean dimethyl ether was stabilized by methane co-flow and combustion respectively. Steady burning of co-flow methane ensured ignition of dimethyl ether/air mixture at temperature ca 330 °C. A detailed reaction mechanism of dimethyl ether low-temperature combustion and methane combustion were applied in the two-dimension axisymmetric numerical simulation. The state-of-the-art low-temperature chemistry of dimethyl ether and methane was applied in numerical simulation. The thermal interaction of flame and solid boundaries was achieved by solid-fluid coupled boundary conditions in numerical simulation. 2D axisymmetric numerical simulation was performed based on the physical measurement and experimental setup. The axial temperature profile of the flame was obtained by experiments and numerical simulation relatively well agreed with the experiment. The chemical radicals, like $OH$, $CH_2O$, and $HO_2$, occurrence in lean dimethyl/air flame were also obtained by experiment. The computational simulation of flame showed that there was thermal interaction between flames and solid parts of the experimental burner. The dimethyl ether/air mixture was preheated upstream by the thermal conductivity of solid parts. High and Low-temperature combustion zones were identified on the base of results of numerical simulation and the presence of radicals specific for the appropriate type of combustion respectively.

## INTRODUCTION

The micro and mesoscale combustion devices like a micro-gas turbine [6, 7], micro swing engine [8], etc. have been researched and developed in the last few years. It was found that there is a problem with the stable flame due to the relatively high heat loss and short residence time of the fuel-oxidizer mixture in the micro combustor. The essential knowledge of premixed and non-premixed combustion characteristics is necessary to the successful design of micro combustion-based energy systems. Dimethyl ether (DME) is considered as a prototype fuel in micro combustion. The future usability of DME is of remarkable importance in the framework of the methanol economy [9]. DME can be produced by the chemical recycling of carbon dioxide. The comprehensive chemical kinetics of

DME oxidation (low and high temperature) including experimental validation has been investigated intensively in the previous two decades [10, 11]. An evident improvement of the rate constants of some key elementary reactions in low-temperature DME oxidation schemes has been achieved even though some uncertainties still exist. The numerical simulation of the ignition, propagation, extinction, and structure of DME flames including the coupling of high-temperature and low-temperature combustion (shortly HTC and LTC, respectively) has enabled on the base of the researched chemical kinetics models. The structural characteristics of the different DME flame regimes, i.e., lean, and rich cool flames, hot flames, and double flames, were described by Ju [3].

## EXPERIMENTAL MEASUREMENT AND METHODS

The experimental system is schematically shown in Fig. 1. The experimental system was based on a burner [4] consisting of a central part with a total of 5031 holes of diameter 0.5 mm in 5 mm thick brass disc (DME/Air) and a co-flow section (Methane/air). The disc was designed for the stabilization of laminar flat flame. The inlet stainless-steel tubes of the burner were covered by insulation (mineral wool) and foil (aluminum). Air for combustion of DME was preheated to ca 300 °C using a flow heater. Preheated air was mixed with DME downstream air heater in T-junction. Four K-type thermocouples (T1-T4) were installed upstream main part of the burner (perforated brass disc) to control the temperature of air and DME/air mixture. Monitoring of temperature was used to avoid unwanted oxidation of DME and flashback phenomena. The actual temperature of the perforated plate (T4) was also used for the interpretation of the experimental measurement because the theoretical presumption for stable low-temperature combustion of DME is ca 330 °C in this case.

The additional heat source was realized by a stoichiometric methane/air steadily combustion in the co-flow section of the burner (an annulus surrounding the central part). Steadily co-flow and combustion of a methane-air mixture also provided energy to achieve the auto ignition of ultra-lean DME/air mixture at temperature ca 330 °C. More details about experimental setup and methods are discussed in [1], which is purely focused on experimental measurement.
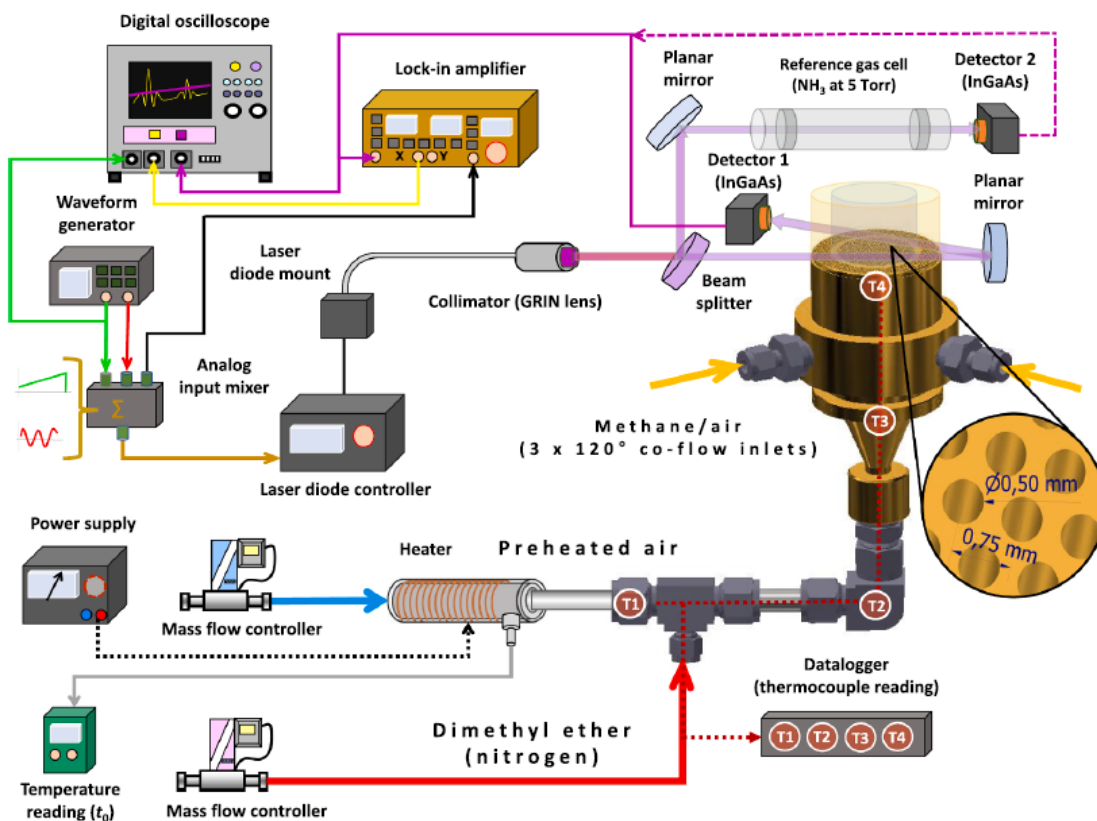


**FIGURE 1.** Schematic of the experimental setup

# NUMERICAL METHODS

To study the combustion characteristics of ultra-lean DME/air mixture and the thermal interaction of the flame of DME and co-combusted Methane, a numerical simulation with detailed chemistry was performed. The numerical simulation was performed as two-dimensional axisymmetric with solid walls thermal coupling. The sketch of the computational domain and boundary conditions are illustrated in Fig. 2.
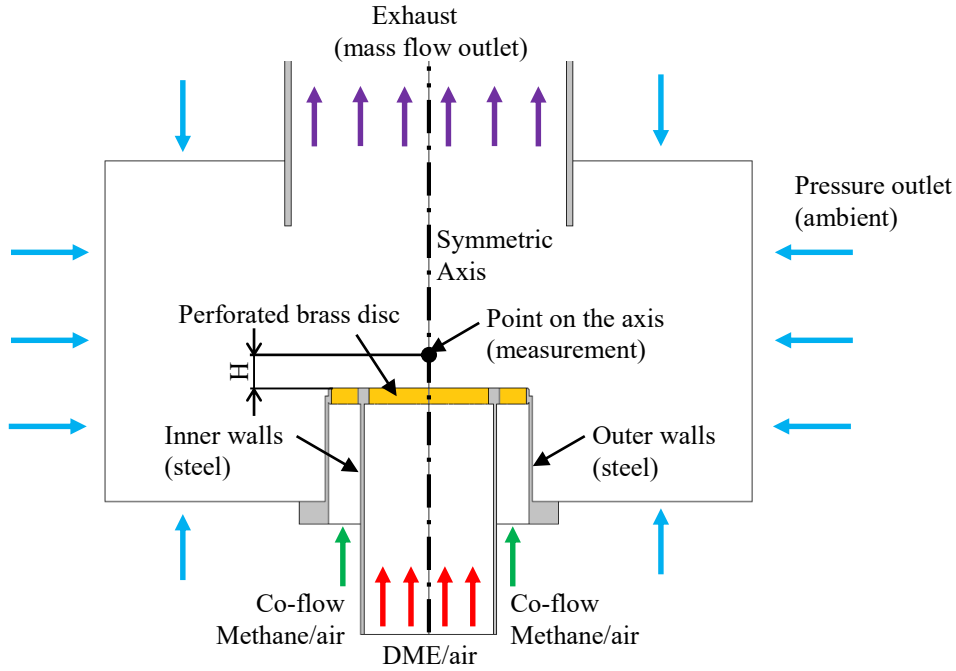


**FIGURE 2.** Physical model, computational domain, and boundary conditions

Pressure outlet was applied at far-field boundaries (ambient). The perforated brass disc was treated as a porous domain, and parameters of the porous zone (porosity and resistance coefficient) were calculated on the base of geometry parameters and analytic calculation. The disc was set as a laminar zone in accordance with the Reynolds number calculated for one hole of the disc. The solid walls of the burner were set as conductive and non-slip. The heat exchanges between solid walls and gases were computed by using coupled boundary conditions. All parameters of simulation were specified and set according to experimental measurement, e.g., mass flow of DME/air mixture, the mass flow of Methane/air mixture, the temperature of the brass disc (T4 thermocouple) et cetera.

The main governing equations of the mathematical model of time steady flow presented in this paper can be easily found in CFD textbooks, e.g., [5]. Nevertheless, the fundamental equations of mass, momentum, energy, and species are shown as follows.

$$\frac{\partial(\rho \cdot u_j)}{\partial x_j} = 0 \tag{1}$$

$$\frac{\partial(\rho \cdot u_i \cdot u_j)}{\partial x_j} = -\frac{\partial p}{\partial x_i} + \frac{\partial}{\partial x_j}\left(\eta \cdot \frac{\partial u_i}{\partial x_j}\right) + \rho \cdot \delta_{i3} \cdot g \tag{2}$$

$$\frac{\partial(\rho \cdot u_j \cdot h_{tot})}{\partial x_j} = \frac{\partial p}{\partial t} + \frac{\partial}{\partial x_j}\left(\lambda \cdot \frac{\partial T}{\partial x_j}\right) + \frac{\partial(u_j \cdot \tau_{jl})}{\partial x_l} + S_{h,rad} + S_{h,chem} \tag{3}$$

$$\frac{\partial(\rho \cdot u_j \cdot Y_i)}{\partial x_j} = \frac{\partial}{\partial x_i}\left(\rho \cdot D_{m,i}\frac{\partial Y_i}{\partial x_j} + D_{T,i}\frac{1}{T}\frac{\partial T}{\partial x_j}\right) + R_i + S_i \tag{4}$$

$$p = \rho \cdot R \cdot T \sum_{i=1}^{n} \frac{Y_i}{M_i} \tag{5}$$

$$h_{tot} = \int_{T_{ref}}^{T} c_p dT + \frac{1}{2}u_j{}^2 - \frac{p}{\rho} \tag{6}$$

where $\rho$ (kg·m$^{-3}$), $p$ (Pa), $T$ (K), $u$ (m·s$^{-1}$), $h$ (J·kg$^{-1}$), $\eta$ (Pa·s), $\lambda$ (W·m$^{-1}$·K$^{-1}$), $c_p$ (J·kg$^{-1}$·K$^{-1}$) and $R$ (J·K$^{-1}$·mol$^{-1}$) are density, pressure, temperature, velocity, enthalpy, dynamic viscosity, thermal conductivity, specific heat capacity, and universal gas constant, next $Y_i$ (kg·kg$^{-1}$), $D_{m,i}$ (m$^2$·s$^{-1}$), $D_{T,i}$ (kg·m$^{-1}$·s$^{-1}$) and $M_i$ (kg·mol$^{-1}$) are mass fraction, diffusion coefficient, thermal diffusion coefficient, and molecular weight of $i^{th}$ species of the mixture. Mixing law was used to the specification of physical properties of the mixture, e.g., viscosity, thermal conductivity, etc. and the kinetic theory was used for calculation of Mass and Thermal diffusivity.

The fundamental equations were solved by using of finite volume method and the numerical computation was achieved by CFD code Fluent 19.3 [14]. The SIMPLE algorithm was used as pressure velocity coupling scheme and Least Squared Cell Based gradient method was used as spatial discretization.
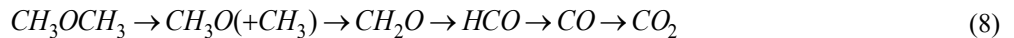
The finite-rate chemistry model with 71 reactions and 26 species was used to solving chemical reactions [2]. Thermodynamics and transport properties were load from the CHEMKIN database. Stiff chemistry solver, full multicomponent diffusion, and thermal diffusion were included in the calculation of chemical reactions.

Turbulent model RNG $k$-$\varepsilon$ with full buoyancy effect and scalable wall functions were used to simulate, and the perforated brass disc was set as a porous laminar zone. The discrete ordinates model and Weighted-Sum of Gray Gas Model were adopted for the calculation of radiation heat transfer. The computation domain had 187 500 cells. The convergence criterion was $1 \cdot 10^{-4}$ except for energy, which was $1 \cdot 10^{-6}$.

## RESULTS AND DISCUSSION

The axial profile of temperature obtained from the thermocouple measurement was compared with the results of numerical simulation see Fig. 3. Thermocouples K and B were used for the measurement of the axial profile. Temperature measured by thermocouples was corrected for radiation heat loss via the procedure provided by [12]. The uncertainties of individual data points were estimated to be ± 25 °C for the K-type thermocouple and ± 50 °C for the B-type thermocouple. Transition of from the cool flame regime to the hot flame regime can be seen because $T_{crit}$ was exceeded in our burner setup with the co-flow flame. ($T_{crit} \approx 540$ °C according to [13]). The hot flame reaction zone with abundant chemiluminescence at $H = 5$ mm can be clearly recognized in Fig. 5a. An important issue arises concerning the interaction of the central flow with the surrounding (co-flow) flame.

As was mentioned in the introduction, we can consider two types of combustion of DME, namely Low-Temperature Combustion (LTC) and High-Temperature Combustion (HTC). It is well known that high temperature combustion of DME proceeds via lumped equations [2]:

$$CH_3OCH_3 \rightarrow CH_3OCH_2 \rightarrow CH_2O(+CH_3) \rightarrow HCO \rightarrow CO \rightarrow CO_2 \tag{7}$$

$$CH_3OCH_3 \rightarrow CH_3O(+CH_3) \rightarrow CH_2O \rightarrow HCO \rightarrow CO \rightarrow CO_2 \tag{8}$$

Low temperature combustion (oxidation) chemical pathway production carbon monoxide from keto-hydroperoxide species (HO$_2$CH$_2$OCHO), given in a lumped form [2]:

$$CH_3OCH_3 \rightarrow HO_2CH_2OCHO \rightarrow CH_2O + CO + 2OH \tag{9}$$
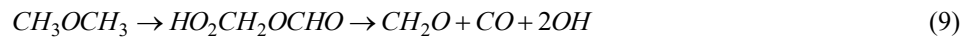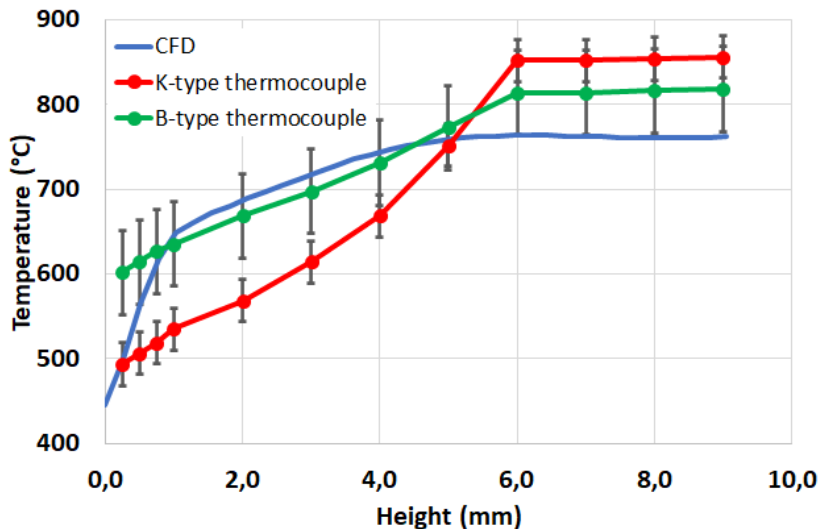
**FIGURE 3.** Axial temperature profiles obtained from the thermocouple measurement compared with results of CFD simulation

According to previous chemical pathways, zones of high and low-temperature combustion can be identified. We can see, thermal interaction of flame and the perforated brass disc caused an additional heat source. It led to thermal dissociation of FME and low-temperature combustion inside holes of the brass disc and close to the top surface of the disc. see Fig. 4a.



(a)



(b)
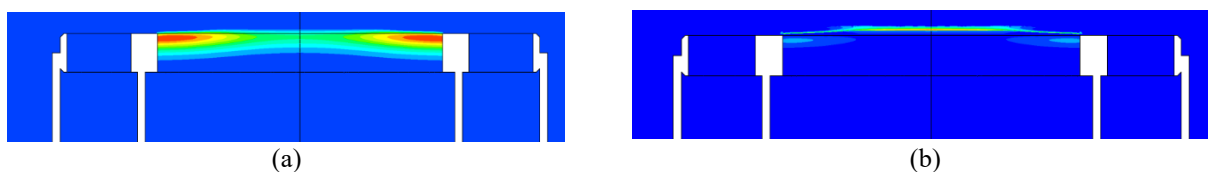
**FIGURE 4.** (a) LTC combustion zone visualized by hydroperoxide species ($HO_2CH_2OCHO$), (b) HTC combustion zone visualized by methoxymethyl radical ($CH_3OCH_2$)

The hot flame reaction zone with abundant chemiluminescence at $H = 5mm$ can be clearly recognized in Fig. 5a. It is so well known that chemiluminescence is related to the presence of radicals in the flame (e.g., $HO_2$, OH etc.).



(a)



(b)
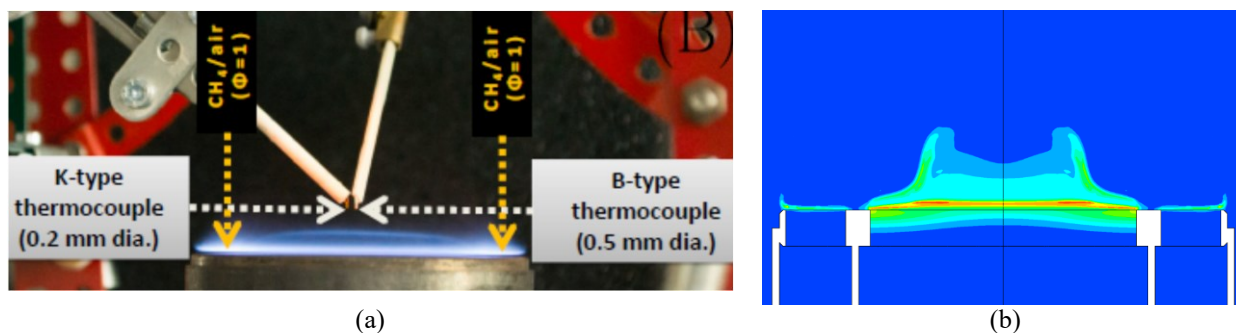
**FIGURE 5.** (a) Illustrative images of thermocouple measurement at the $H = 9$ mm, (b) mass fraction of $HO_2$ radical illustrates chemiluminescence phenomena

Mass fraction of $HO_2$ radical is shown in Fig. 5b. We can see a relatively good comparison between experimental measurement and CFD simulation, but the illumination of flame is a very complicated phenomenon, and it is caused by more than $HO_2$ radical.

# CONCLUSION

The combustion of preheated ultra-lean dimethyl ether/air mixture was investigated numerically in this paper. Two regimes of DME combustion were identified by CFD simulation in accordance with experimental measurement. Heat transfer and possibly also the transport of reactive species (e.g., OH radicals) from the post-combustion region of the $CH_4$/air flame could play a role in the evolution of the hot flame regime. Thermal interaction of flame and top surface of causes thermal dissociation of DME and low temperature combustion inside holes of performed brass disc. 3D Numerical simulations of fluid flow based on the LES turbulence model with detailed chemistry in a realistic burner geometry, which would take real effects into account, are in preparation considering the approach already used for modelling DME/air premixed cool flames.

# ACKNOWLEDGMENTS

# REFERENCES

1. V. Nevrlý, M. Dostál, V. Klečka, P. Bitala, V. Válek, M. Vašinek, T. Blejchař, J. Suchánek, Z. Zelinger and J. Wild, TDLAS-based in situ diagnostics for the combustion of preheated ultra–lean dimethyl ether/air mixtures. Fuel. **263,** 116652 (2020).
2. R. S. Khare, S. K. Parimalanathan, V. Raghavan, and K. Narayanaswamy, A comprehensively validated compact mechanism for dimethyl ether oxidation: an experimental and computational study. Combust Flame. **196**, 116–28 (2018).
3. Y. Ju, On the propagation limits and speeds of premixed cool flames at elevated pressures. Combust Flame. **178** 61–9 (2017).
4. G. Hartung, J. Hult and C. F. Kaminski, A flat flame burner for the calibration of laser thermometry techniques. Meas Sci Technol. **17** (9), 2485–93 (2006).
5. J. D. Anderson Jr., *Computational Fluid Dynamics. The Basics with Applications*, McGraw-Hill, USA, 1995.
6. K. Maruta, Micro and mesoscale combustion, Proc. Combust. Inst. **33** (1) 125–150 (2011).
7. A. H. Epstein, Millimeter-scale, micro-electro-mechanical systems gas turbine engines, J. Eng. Gas Turb. Power. **126** (2) 205–226 (2004).
8. W. Dahm, J. Ni, K. Mijit, R. Mayor, G. Qiao, A. Benajmin, et al., Micro internal combustion swing engine (MICSE) for portable power generation systems. Ann Arbor. 1050 (2001), pp. 42140–48109.
9. A. Álvarez, A. Bansode, A. Urakawa, A. V. Bavykina, T. A. Wezendonk, M. Makkee, et al. Challenges in the greener production of formates/formic acid, methanol, and DME by heterogeneously catalyzed $CO_2$ hydrogenation processes. Chem Rev. **117** (14) 9804–38 (2017).
10. E. W. Kaiser, T. J. Wallington, M. D. Hurley, J. Platz, H. J. Curran, W. J. Pitz, et al. Experimental and modeling study of premixed atmospheric-pressure dimethyl ether - air flames. J Phys Chem A. **104** (35) 8194–206 (2000).
11. Z. Zhao, M. Chaos, A. Kazakov and F. L. Dryer, Thermal decomposition reaction and a comprehensive kinetic model of dimethyl ether. Int J Chem Kinet. **40** (1)1–18 (2008).
12. W. Weng, J. Borggren, B. Li, M. Aldén and Z. Li, A novel multi-jet burner for hot flue gases of wide range of temperatures and compositions for optical diagnostics of solid fuels gasification/combustion. Rev Sci Instrum. **88** (4) 045104 (2017).
13. Y. Ju, C. B. Reuter and S. H. Won, Numerical simulations of premixed cool flames of dimethyl ether/oxygen mixtures. Combust Flame **162** (10) 3580–8 (2015).
14. *ANSYS Fluent Theory Guide*, ANSYS, Inc., 275 Technology Drive Canonsburg, PA 15317.